

# A Close-Coupling Study of Vibrational-Rotational Quenching of CO by collision with Hydrogen Atoms

Benhui Yang\* and P. C. Stancil†

*Department of Physics and Astronomy and the Center for Simulation Physics  
The University of Georgia, Athens, GA, 30602-2451*

N. Balakrishnan‡

*Department of Chemistry, The University of Nevada, Las Vegas, Nevada 89154*

(Dated: July 7, 2005)

## Abstract

Quantum mechanical scattering calculations were performed for the rovibrational relaxation of CO in collisions with H atoms using the close-coupling approach for collision energies between  $10^{-6}$  and  $1500 \text{ cm}^{-1}$ . We adopted the H-CO interaction potential of Werner, Keller, and Schinke and computed state-to-state and total cross sections for the quenching of the  $v=1$ ,  $j=0-2$  levels of CO. Numerous resonances, as a consequence of the van der Waals potential, are observed and the cross sections are found to approach the Wigner limit at low energies. Also, by averaging the cross sections over a Boltzmann distribution of velocities of the incoming atom, quenching rate coefficients are obtained and found to be consistent with previous infinite order sudden approximation calculations for temperatures between 100 and 300 K.

---

\*Electronic address: yang@physast.uga.edu

†Electronic address: stancil@physast.uga.edu

‡Electronic address: naduvala@unlv.nevada.edu

## I. INTRODUCTION

Advanced atmospheric modeling and spectral synthesis of extrasolar giant planets (EGPs), brown dwarfs (BDs), and other cool astrophysical environments requires an extensive array of accurate molecular data if it is to be done reliably. A large portion of the data are either currently unavailable (as the requisite experiments or calculations have not been carried out) or the available data are insufficient to meet the demands required by the modeling applications. Inherent in the majority of model atmosphere/synthetic spectra studies is the assumption of local thermodynamic equilibrium (LTE), i.e. that the level populations of the atoms and molecules can be described by a Boltzmann distribution. There is reason to suspect departure from LTE in EGPs and BDs due to a low abundance of electrons and the strong irradiation from their companion stars. However, non-LTE (NLTE) calculations require cross sections due to collisions with H, He, and H<sub>2</sub>. In this current study, we have begun to address this issue by considering H-CO, a benchmark collision system for this type of process.

The calculation of molecular collisional excitation cross sections has both molecular structure and scattering components. State of the art calculations involve *ab initio* electronic potential energy surface calculations involving large configuration-interaction quantum chemistry codes, and the close-coupled solution of the nuclear scattering equations on these surfaces, including at a minimum all energetically allowed, i.e. open bound rotational-vibrational (RV) levels. For highly excited RV levels, the vibrational continuum may also be required. Both of these components involve significant computational effort.

Carbon monoxide is a well studied molecule, which has been observed in the first detected brown dwarf GL 229B and LTE spectral models suggest its abundance is about 1000 times larger than expected from local chemical equilibrium models [1]. Further, the formyl radical, HCO, is an important intermediary in atmospheric [2], combustion [3], and interstellar chemical reactions [4]. Collision energy transfer dynamics between hydrogen atoms and CO molecules has been the subject of numerous theoretical investigations [5–17]. Theoretical studies on this system have also been sparked by the availability of *ab initio* potential energy surfaces [7, 14]. From the experimental point of view, CO has become a convenient candidate for studies of excitation in collisions with hot hydrogen [18–22]. The experimental attraction is that the hydrogen atoms can be produced by laser photodissociation of HBr, for example.

To date, impressive progress has been made in the construction of potential energy surfaces (PESs) for H-CO. Most of the theoretical scattering work has used the BBH potential [7], which is an early *ab initio* potential energy surface for the HCO system constructed by Bowman, Bittman, and Harding. It provides a generally valid description of the true potential energy surface and the intra- and intermolecular dynamics of this system. Nevertheless, the BBH surface is not sufficiently accurate to reproduce the most recent and the most detailed stimulated emission pumping (SEP) experimental data [14, 22].

More recently, a completely new global PES was constructed by Keller *et al.* [14] based on the *ab initio* calculation of Werner *et al.* [13] (WKS). The WKS potential is a significant step forward in quantitative modeling of the H+CO system. The resonance energies and widths calculated using the WKS potential for HCO and DCO agree well with experiment, and noticeably better than those obtained from the older BBH potential [14]. So, we adopt the WKS potential for this work.

Theoretical calculations for RV excitation have been used to obtain rate coefficients needed to interpret astrophysical data, and the present work is part of a project aimed at calculating the required rate coefficients for CO excited by hydrogen atoms. Estimates of vibrational quenching rate coefficient for CO collisions with H have been made by Scoville *et al.* [23] based on the measurements of von Rosenberg *et al.* [24] and by Ayres and Wiedemann [25] based on the measurements of Glass and Kironde [26]. We report in the present work the results of quantum close-coupling calculations of the rovibrational integral cross sections for CO scattering with H on the WKS potential. Also, by averaging the cross sections over a Boltzmann distribution of velocities of the incoming atom, the quenching rate coefficients are obtained.

This paper is organized as follows: Section 2 gives a brief review of the theoretical methodologies used in the current study. The results of the calculations and discussion of the results are given in Section 3, and Section 4 concludes.

## II. COMPUTATION METHODOLOGY

### A. Quantum Close-Coupling Method

In this section we briefly outline the quantum close-coupling method used in the present calculations of the excitation of CO by H atoms. The reader is referred to Ref. [27] for more detailed discussions of the methodology. The quantum close-coupling equations were introduced into the field of molecular collisions in 1960 by Arthurs and Dalgarno [28] and extended by others [29, 30].

The Hamiltonian for the H-CO system can be written as

$$\hat{H} = \hat{H}_{\text{CO}} - \frac{1}{2\mu} \nabla_R^2 + V(r, R, \theta) \quad (1)$$

where  $r$  is the distance between the carbon and oxygen atom,  $R$  is the distance from the CO center of mass to the H atom, and  $\mu$  is the reduced mass of the hydrogen atom with respect to CO.  $H_{\text{CO}} = -\frac{1}{2m} \nabla_r^2 + v(r)$  is the vibration-rotation Hamiltonian for the isolated CO molecule, where  $m$  is the reduced mass of CO. Its eigenfunctions are products of rotational wave functions  $Y_{jm_j}$  and vibrational wave functions  $\chi_{vj}(r)$ ,  $v(r)$  is the CO diatomic potential,  $j$  and  $m_j$  are the rotational quantum number and its projection on the space-fixed axis. The vibrational wave functions depend only on  $r$ . It is labeled by  $j$  and vibrational quantum number,  $v$ , because the rotation of the CO adds a centrifugal term to the effective vibrational potential. In Eq. (1), the kinetic energy of the relative collision motion can be separated into a radial term and an orbital angular momentum term. The H-CO interaction potential is expressed by  $V(r, R, \theta)$  where  $\theta$  is the angle between  $r$  and  $R$ . The total scattering wave function of the H-CO complex is expanded in terms of functions for radial and angular coordinates. Substitution of the total wave function into the stationary Schrödinger equation with the total Hamiltonian of the H-CO system results in coupled second-order differential equations, where the coupling is represented by matrix elements of the intermolecular potential.

The rovibrational eigenfunctions of isolated CO vibrating rotors were obtained by expanding in a basis set of Hermite polynomials. The vibrational wave function  $\chi(r)$  as well as the rovibrational energy levels  $\epsilon_{vj}$  of the CO molecule are determined numerically by

solving the radial  $r$  nuclear Schrödinger equation:

$$\left[ -\frac{\hbar^2}{2m} \frac{d^2}{dr^2} + \frac{j(j+1)}{2mr^2} + v(r) - \epsilon_{vj} \right] \chi(vj|r) = 0. \quad (2)$$

It is convenient to adopt the total angular momentum representation introduced by Arthurs and Dalgarno [28] where the total angular momentum  $\mathbf{J}$ , is composed of the angular momentum of the CO molecule  $\mathbf{j}$ , and the orbital angular momentum of the collision complex  $\mathbf{l}$ :  $\mathbf{J} = \mathbf{l} + \mathbf{j}$ . Then the coupled equations become block diagonal in  $J$  and independent of its projection on the spaced-fixed axis,  $M$ . Asymptotic solution of the Schrödinger equation yields the scattering  $S$  matrix which contains all the relevant information about H-CO scattering. The total cross sections for transitions from an initial rotational-vibrational state labeled by  $vj$  to a final rotational-vibrational state labeled  $v'j'$  can be expressed in terms of the scattering matrix,  $S$ ,

$$\sigma_{vj \rightarrow v'j'}(E_{vj}) = \frac{\pi}{(2j+1)k_{vj}^2} \sum_{J=0} (2J+1) \sum_{l=|J-j|}^{J+j} \sum_{l'=|J-j'|}^{J+j'} |\delta_{jj'} \delta_{ll'} \delta_{vv'} - S_{jj' ll' vv'}^J|^2, \quad (3)$$

where  $k_{vj} = \sqrt{2\mu(E - \epsilon_{vj})}/\hbar$  is the wave vector in the incoming channel and  $E$  the total energy.

The total vibrational quenching or de-excitation cross section as a function of collision energy  $E_{vj} = E - \epsilon_{vj}$  from a given initial state is obtained as:

$$\sigma_{vj}^{\text{in}}(E_{vj}) = \sum_{v' \neq v, j'} \sigma_{vj \rightarrow v'j'}(E_{vj}), \quad (4)$$

where the summation includes only vibrationally inelastic transitions, but excludes purely elastic vibrational transitions. By integrating the collision energy dependence of the cross sections with a Maxwell-Boltzmann distribution of velocities of the incident atom, the quenching rate coefficients are given by

$$r_{vj}(T) = \left( \frac{8k_B T}{\pi \mu} \right)^{1/2} \frac{1}{(k_B T)^2} \int_0^\infty \sigma_{vj}^{\text{in}}(E_{vj}) \exp(-E_{vj}/k_B T) E_{vj} dE_{vj}, \quad (5)$$

where  $k_B$  is the Boltzmann constant and  $T$  is the temperature.

## B. Potentials

The WKS potential is given by an analytical expression in the two stretching coordinates  $R_{\text{CO}} = r$ ,  $R_{\text{HC}}$ , and the HCO bending angle  $\alpha$ . It involves 230 linear and 129 nonlinear

parameters, which were determined by fitting of about 1000 points from *ab initio* electronic structure calculations. The ground-state PES has a complicated overall topology. It has two wells, the main one with a minimum of 0.8339 eV at  $R_{\text{HC}} = 2.110 a_0$ ,  $R_{\text{CO}} = 2.233 a_0$ , and  $\alpha \approx 124.5^\circ$ ; the secondary one is near  $\alpha \approx 30^\circ$  [13, 14].

For the convenience of calculations, the potential  $V(r, R, \theta)$  may be expanded in the form:

$$V(r, R, \theta) = \sum_{\lambda} v_{\lambda}(r, R) P_{\lambda}(\cos(\theta)) \quad (6)$$

where  $P_{\lambda}$  is the Legendre polynomial. The quantum close coupling scattering calculations were performed by expanding the angular dependence of the potential in Legendre polynomials up to order 20. A 15-point Gauss-Hermite quadrature over  $r$  was used to represent the vibrational wavefunctions while a 22 point quadrature in the angular coordinate was used to project out the Legendre expansion coefficients, the latter being the number of points for the theta integration to obtain the potential matrix. Convergence testing was performed to ensure the reliability of the results, for both total quenching and state-to-state transitions, with the largest calculations including a Legendre polynomial expansion of the potential up to order 35 and 36 quadrature points for the angular integration.

### III. RESULTS AND DISCUSSION

Calculations were done with the molecular scattering program MOLSCAT [32] to generate integral state-to-state cross sections. The coupled-channel equations were integrated using the modified log-derivative Airy propagator of Alexander and Manolopoulos [33] with a variable step size. The wave function was propagated to a maximum intermolecular separation of  $R = 100 \text{ \AA}$ . Calculations were performed for collision energies between  $10^{-6} \text{ cm}^{-1}$  and  $1500 \text{ cm}^{-1}$  in order to present accurate thermally averaged rate constants from  $10^{-5}$  to 300 K. At each energy a sufficient number of total angular momentum partial waves has been included to secure convergence of the cross sections. The maximum value of  $J$  employed in the calculation was 60. The basis set used consisted of 36 rotational states in the ground vibrational state of CO, 31 rotational levels of  $v = 1$ , and 21 states in the vibrational closed channel,  $v = 2$ , or B2(35,30,20) in the notation of Ref. [15].

## A. Cross Sections

We have performed calculations of the collision energy dependence of state-to-state cross sections for three initial rovibrational states ( $v = 1, j = 0, 1, \text{ and } 2$ ) for the de-excitation of CO by H on the WKS surface.

Examples of the state-to-state cross sections for quenching of the  $v = 1, j = 0, 1, \text{ and } 2$  rotational levels into the individual final rotational levels ( $j'=0, 1, 2, 3, 4, 5, 10, 20$ ) of the  $v = 0$  vibrational state are shown in Figs. 1, 2, and 3, respectively. Generally, the state-to-state cross sections from the different initial  $j$  levels have similar structure. Each of the cross sections decreases initially and exhibits the threshold behavior predicted by Wigner's Law [34, 35]. The cross sections reflect the presence of a large number of shape resonances at higher energies which will influence the quenching rate coefficients. Above the van der Waals region, a number of resonance structures are also evident due to the opening of closed channels in the rotational manifold of the initial vibrational state  $v = 1$ . These are displayed as insets to Figs. 1, 2, and 3 for collision energies of 10 to 100  $\text{cm}^{-1}$ . The locations of the  $j$  thresholds are marked in the insets and clearly align with the resonances which, however, are not completely resolved due to long computational times at these collision energies. Resonances are shown for  $j$  starting at 2 or 3 as the lower  $j$  resonances are lost in the forest of van der Waals resonances at lower energies. For example, for the initial channel of  $v = 1, j = 0$ , the  $j = 1$  threshold occurs at 3.78  $\text{cm}^{-1}$ . The strong resonance in Figs. 1 and 2 at 0.16  $\text{cm}^{-1}$  is found to be due to the  $l = 2$  partial wave. It is seen to decrease from  $j = 0$  to  $j = 1$  and is not evident by  $j = 2$  presumably due to the low height of the  $l = 2$  potential barrier. A similar decrease of shape resonance strength with increasing  $j$  was calculated by Zhu *et al.* [36] for vibrational quenching of  $v = 1$  in He-CO collisions.

By using Eq. (4) the cross-sections from each initial rovibrational state of CO are summed over all final rotational states to obtain the total vibrational quenching cross sections as a function of relative translational energy. Fig. 4 depicts the comparison of the total quenching cross sections from  $v = 1, j = 0, 1, \text{ and } 2$  to  $v' = 0$ . The results show qualitatively similar structure with a number of resonances in the energy range between 0.1 and 10  $\text{cm}^{-1}$ , like those shown in Figs. 1, 2, and 3 for the state-to-state cross sections. At low energies where only  $s$ -wave scattering contributes, the cross sections vary inversely as the relative velocity. For the present system, the Wigner limit is reached for incident energies lower than 0.001

$\text{cm}^{-1}$  as required by Wigner's law. For energies higher than  $100 \text{ cm}^{-1}$  the cross sections increase with increasing collision energy, typical of vibration-translation/rotation energy transfer. In the intermediate energy region between  $10^{-1}$  and  $100 \text{ cm}^{-1}$  the cross sections display an oscillatory structure due to shape resonances supported by the van der Waals interaction potential. As discussed by Reid *et al.* [37], the low collision energy regime fosters the formation of metastable or van der Waals complexes. These long lived complexes allow multiple collisions to occur and may strongly enhance the vibrational relaxation process and influence the open-channel (shape) [38] and closed-channel (Feshbach)[39] resonances.

## B. Rotational Distribution

Figs. 5-8 present the distributions of final rotational levels in the  $v' = 0$  level from the quenching of  $v = 1, j=0, 1,$  and  $2$  levels at different collision energies. The distributions are similar for all energies lower than  $10^{-2} \text{ cm}^{-1}$ . The final rotational distribution is broad and centered in the region of low  $j'$  levels. The oscillatory behavior of the distributions is due to the competition between even and odd order terms in the Legendre polynomial expansion of the interaction potential. The distributions reach out to higher rotational levels  $j'$  as the collision energy increases. One can see that for the quenching from  $v = 1, j = 0, 1,$  and  $2$ , a significant fraction of the vibrational energy is transferred to final rotational energy as shown by the rotational distributions. Fig. 6 shows the final rotational distribution in the  $v' = 0$  level from the quenching of  $v = 1, j = 0$  level at collision energy  $E = 0.16 \text{ cm}^{-1}$ , which corresponds to the largest shape resonance shown in Fig. 1. It can be seen that the distribution is dominated by  $\Delta j = 1$ , quite different from that shown in Fig.5. At higher energies, the final rotational distribution is broad and flat, this is because only  $s$ -wave scattering contributes in the incident channel at  $10^{-5} \text{ cm}^{-1}$ , whereas at higher energies the contribution from a number of higher angular momentum partial waves leads to a broader distribution of rotational levels in the outgoing channel.

Lee and Bowman [40, 41] using the BBH potential noted a propensity for even  $\Delta j$  transitions in their study of rotational excitation of CO due to H collisions. This propensity occurred for collision energies significantly below a resonance position while the opposite propensity, i.e. odd  $\Delta j$  was seen for energies above the resonance. However, at resonance no propensity was evident. While we also find no propensity near a resonance, the  $0.16 \text{ cm}^{-1}$

feature for example, the lack of a clear even or odd  $\Delta j$  propensity off-resonance may be related to differences in the BBH and WKS potentials. We will explore this discrepancies in a future publication.

### C. Rate Coefficients

As expressed in Eq. (5), the total quenching cross sections are thermally averaged over the kinetic energy distribution to give rate coefficients from specific initial rovibrational states of CO at a temperature  $T$ . We calculated the quenching rate coefficients for initial rovibrational states ( $v = 1, j = 0, 1, \text{ and } 2$ ). They are shown in Fig. 9 for temperatures ranging from  $10^{-5}$  to 300 K. From Fig. 9, it can be seen that below the temperature of about  $10^{-3}$  K, where the rate coefficient become constant, the Wigner regime has set in. Between  $10^{-3}$  and 50 K, which is the van der Waals interaction-dominated regime, the rate coefficients exhibit unusual temperature dependence. Finally, it is shown that at temperatures above 50 K the rate coefficients increase with increasing temperature. Note that the humps of the rate coefficient curves are due to the presence of shape resonances as was indicated previously for the cross sections in Figs. 1-4. With the increase in rotational excitation, the resonances become suppressed and their effect becomes less prominent in the rate coefficients. In addition, as the temperature decreases, the curves for  $j = 0, j = 1,$  and  $j = 2$  behave differently, but each eventually attains a finite limiting value as the temperature approaches zero, in agreement with Wigner's Law. Generally, at temperatures below about 10 K, the rate coefficients show an increase with initial rotational excitation until they begin to approach the ultra cold limit below  $\sim 10^{-2}$  K. At higher temperature, the rate coefficients increase monotonously, then finally converge.

In the inset of Fig. 9, the close-coupling rate coefficients are compared with the infinite order sudden (IOS) approximation results for vibrational quenching from Balakrishnan *et al.* [17] for  $v = 1 \rightarrow v = 0$ . At 100 K, the present results are smaller than the IOS calculation, while excellent agreement is evident at 200 K and 300 K. The small discrepancy, we believe is due to two issues: 1) the approximations in the IOS method and 2) in the IOS approximation, the rate coefficient for the vibrational transition  $v \rightarrow v'$  is given [27]

$$r_{v \rightarrow v'} = \sum_{j'} r_{v0 \rightarrow vj'} \quad (7)$$

where  $r_{v0 \rightarrow v'j'}$  is the state-to-state rate coefficient for transitions from rovibrational state  $v, j = 0$  to rovibrational state  $v', j'$ . From Eq. (7), it can be seen that the quenching rate coefficients calculated in the current work from initial states  $v = 1, j=0, 1$ , and 2, cannot be directly compared with those obtained using IOS approximation. However, the reasonable agreement does suggest that the IOS method is a valid approximation at high temperatures when rotational selectivity is not needed.

#### D. Pure rotational quenching

In Figs. 10 and 11, pure rotational quenching cross sections and rate coefficients, respectively, are presented for  $v = 1, j = 1$  and  $j = 2$ . The pure rotational cross sections and rate coefficients are significantly larger than the pure vibrational results as expected (see for example Bodo, Gianturco, and Dalgarno [42]) and they approach the Wigner regime at the lowest energies and temperatures. In this limit it is seen that the cross sections and rate coefficients are largest for  $\Delta j = -1$  transitions in agreement with the trends found by Florian, Hoster, and Forrey [43] for He-CO.

For the higher temperatures of 5-100 K, the rate coefficients are very similar to those for pure rotational quenching in  $v = 0$  as reported by Balakrishnan *et al.* [17].

#### E. Astrophysical implications

In astrophysical environments, the coolest temperatures are typically about 10 K which are found in the dense cores of star-forming regions. However, the lowest assessable temperature is that set by the temperature of the cosmic microwave background (CMB): 2.73 K at the current redshift, but higher at larger redshifts. While the rate coefficients for pure rotational quenching in both  $v = 0$  [17] and  $v = 1$ , as shown in Fig. 11, are fairly constant (though the results in Fig. 11 peak near 5 K for  $j = 2$ ), the vibrationally quenching rate coefficients for  $v = 1$  have local minima near 30 K and increase ( $j = 1$ ) or are flat for lower temperatures. Typical extrapolations of IOS rate coefficients, such as those given by Balakrishnan *et al.* [17] which were computed down to 100 K, or from the experiments of Glass and Kironde [26] which are measured down to 840 K, adopt a Landau-Teller form which has a temperature dependence proportional to  $T \exp(-a/T^{1/3})$  where  $a$  is a constant

related to the collider (see for example González-Alfonso *et al.* [44]). The use of such fits for temperatures typical of dense cores would overestimate the vibrational quenching rate coefficients by an order of magnitude. The error is reduced somewhat at the CMB temperature, while at 300 K, the relation given by Ref. [44] gives a value of  $1.9 \times 10^{-12} \text{ cm}^3\text{s}^{-1}$ , somewhat larger than the current values shown in Fig. 11. It is therefore important to have explicitly computed or measured rate coefficients at these low temperatures.

#### IV. SUMMARY AND CONCLUSIONS

Vibrational and rotational quenching of the H-CO system has been studied using an explicit quantum mechanical close-coupling approach on the WKS surface. Both state-to-state and total quenching cross sections from  $v = 1$ ,  $j=0, 1$ , and 2 show resonance structures at intermediate energies due to the van der Waals well. From the distributions of final rotational levels in  $v = 0$  due to the quenching of  $v = 1$ ,  $j = 0, 1$ , and 2 levels, a significant fraction of the vibrational energy is found to be transferred to rotational energy. The quenching rate coefficients attain finite values in the limit of zero temperature in accordance with quantum mechanical threshold laws. Comparison with IOS rate coefficients shows reasonable agreement.

#### Acknowledgments

BHY and PCS acknowledge support from NASA grant NNG04GM59G. NB acknowledges support from NSF through grant PHY-0245019. Some of the calculations were performed on the IBM p655 High Performance Computer of the UGA RCC.

- 
- [1] K.S. Noll, T.R. Geballe, and M.S. Marley, *Astrophys. J.* **489**, L87 (1997).
  - [2] B. J. Finlayson-Pitts and J. N. Pitts, Jr., *Atmospheric Chemistry: Fundamentals and Experimental Techniques* (Wiley and Sons, New York, 1986), and references therein.
  - [3] W. C. Gardiner, Jr., *Combustion Chemistry* (Springer-Verlag, New York, 1984), and references therein.
  - [4] S. Chu and A. Dalgarno, *Proc. Roy. Soc.* **342**, 194 (1975).

- [5] S. Green and P. Thaddeus, *Astrophys. J.* **205**, 766 (1976).
- [6] T. H. Dunning, *J. Chem. Phys.* **73**, 2304 (1980).
- [7] J. M. Bowman, J. S. Bittman, and L. B. Harding, *J. Chem. Phys.* **85**, 911 (1986).
- [8] H. Romanowski, K. T. Lee, J. M. Bowman, and L. B. Harding, *J. Chem. Phys.* **84**, 2520 (1986).
- [9] L. C. Geiger, G. C. Schatz, and L. B. Harding, *Chem. Phys. Lett.* **114**, 520 (1985).
- [10] B. Gazdy, J. M. Bowman, and Q. Sun, *Chem. Phys. Lett.* **148**, 512 (1988).
- [11] B. Gazdy, J. M. Bowman, S-W. Cho, and A. F. Wagner, *J. Chem. Phys.* **94**, 4192 (1991).
- [12] D. Wang and J. M. Bowman, *J. Chem. Phys.* **100**, 1021 (1994); B. Gazdy and J. M. Bowman, *Adv. Mol. Vib. Collision Dyn.* **1B**, 105 (1991).
- [13] H.-J. Werner, C. Bauer, P. Rosmus, H.-M. Keller, M. Stumpf, and R. Schinke, *J. Chem. Phys.* **102**, 3593 (1995).
- [14] H.-M. Keller, H. Floethmann, A. J. Dobbyn, R. Schinke, H.-M. Werner, C. Bauer, and P. Rosmus, *J. Chem. Phys.* **105**, 4983 (1996).
- [15] S. Green, B. Pan, and J.M. Bowman, *J. Chem. Phys.* **102**, 8800 (1995).
- [16] S. Green, H.-M. Keller, R. Schinke, and H.-M. Werner, *J. Chem. Phys.* **105**, 5416 (1996).
- [17] N. Balakrishnan, M. Yan, and A. Dalgarno, *Astrophys. J.* **568**, 443 (2002).
- [18] C. F. Wood, G. W. Flynn, and R. E. Weston, Jr., *J. Chem. Phys.* **77**, 4776 (1982).
- [19] C. A. Wight and S. R. Leone, *J. Chem. Phys.* **78**, 4875 (1983); **79**, 4823 (1983).
- [20] G. K. Chawla, G. C. McBane, P. L. Houston, and G. C. Schatz, *J. Chem. Phys.* **88**, 5481 (1988).
- [21] G. C. McBane, S. H. Kable, P. L. Houston, and G. C. Schatz, *J. Chem. Phys.* **94**, 1141 (1991).
- [22] J. D. Tobiasson, J. R. Dunlop, and E. A. Rohlfing, *J. Chem. Phys.* **103**, 1448 (1995).
- [23] N. W. Scoville, R. Krotkov, and D. Wang, *Astrophys. J.* **240**, 929 (1980).
- [24] C. W. von Rosenberg, R. L. Taylor, and J. D. Teare, *J. Chem. Phys.* **54**, 1974 (1971).
- [25] T. R. Ayres and G. R. Wiedemann, *Astrophys. J.* **338**, 1033 (1989).
- [26] G. P. Glass and S. Kironde, *J. Chem. Phys.* **86**, 908 (1982).
- [27] D. Flower, *Molecular Collisions in the Interstellar Medium* (Cambridge University Press, Cambridge, 1990), and references therein.
- [28] A. Arthurs and A. Dalgarno, *Proc. Roy. Soc. (London Ser.)* **A256**, 540 (1960).
- [29] W. A. Lester, Jr., *Meth. Comput. Phys.* **10**, 211 (1971).

- [30] D. Secrest, in *Atom-Molecule Collision Theory: A Guide for the Experimentalist*, edited by R. B. Bernstein (Plenum, New York, 1979).
- [31] S. Green, *J. Chem. Phys.* **70**, 4686 (1979).
- [32] J. M. Hutson and S. Green, MOLSCAT computer code, version 14 (1994), distributed by Collaborative Computational Project No. 6 of the Engineering and Physical Sciences Research Council (UK).
- [33] M. H. Alexander and D. E. Manolopoulos, *J. Chem. Phys.* **86**, 2044 (1987).
- [34] E. P. Wigner, *Phys. Rev.* **73**, 1002 (1948).
- [35] N. Balakrishnan, V. Kharchenko, R. C. Forrey, and A. Dalgarno, *Chem. Phys. Lett.* **80**, 3224 (1997).
- [36] C. Zhu, N. Balakrishnan, and A. Dalgarno, *J. Chem. Phys.* **115**, 1335 (2001).
- [37] J. P. Reid, C. J. S. M. Simpson, and H. M. Quiney, *J. Chem. Phys.* **107**, 9929 (1997).
- [38] J. P. Toennies, W. Welz, and G. Wolf, *J. Chem. Phys.* **71**, 614 (1979).
- [39] D. A. Micha, *Phys. Rev.* **162**, 88 (1967).
- [40] K.-T. Lee and J. M. Bowman, *J. Chem. Phys.* **85**, 6225 (1986).
- [41] K.-T. Lee and J. M. Bowman, *J. Chem. Phys.* **86**, 215 (1987).
- [42] E. Bodo, F. A. Gianturno, and A. Dalgarno, *Chem. Phys. Lett.* **353**, 127 (2002).
- [43] P. M. Florian, M. Hoster, and R. C. Forrey, *Phys. Rev. A* **70**, 032709 (2004).
- [44] E. González-Alfonso, C. M. Wright, J. Cernicharo, D. Rosenthal, A. M. S. Boonman, and E. F. van Dishoeck, *Astron. Astrophys.* **386**, 1074 (2002).

## Figure Captions

- Fig. 1. State-to-state integral cross sections for H+CO as a function of collision energy from  $v = 1, j = 0$  to  $v' = 0, j'$ : solid line  $-j' = 0$ , dotted line  $-j' = 1$ , open circle with line  $-j' = 2$ , solid square with line  $-j' = 3$ , solid triangle with line  $-j' = 5$ , star with line  $-j' = 10$ , solid circle with line  $-j' = 20$ . The solid squares in inset denote rotational energies of the openings of rotational level  $j=2, 3, 4, 5, 6$  in the  $v = 1$  vibrational level.
- Fig. 2. State-to-state integral cross sections for H+CO as a function of collision energy from  $v = 1, j = 1$  to  $v' = 0, j'$ : solid line  $-j' = 0$ , dotted line  $-j' = 1$ , open circle with line  $-j' = 2$ , solid square with line  $-j' = 3$ , solid triangle with line  $-j' = 5$ , star with line  $-j' = 10$ , solid circle with line  $-j' = 20$ . The solid squares in inset denote rotational energies of the openings of rotational level  $j=3, 4, 5, 6$  in the  $v = 1$  vibrational level.
- Fig. 3. State-to-state integral cross sections for H+CO as a function of collision energy from  $v = 1, j = 2$  to  $v' = 0, j'$ : solid line  $-j' = 0$ , dotted line  $-j' = 1$ , open circle with line  $-j' = 2$ , solid square with line  $-j' = 3$ , solid triangle with line  $-j' = 5$ , star with line  $-j' = 10$ , solid circle with line  $-j' = 20$ . The solid squares in inset denote rotational energies of the openings of rotational level  $j=3, 4, 5, 6, 7$  in the  $v = 1$  vibrational level.
- Fig. 4. Cross section for the total vibrational quenching of the  $v = 1, j=0, 1$  and  $2$  levels of CO in collisions with H as a function of collision energy. solid line with star  $-j = 0$ , solid line with open circle  $-j = 1$ , solid line with open triangle  $-j = 2$ .
- Fig. 5. Distributions of final rotational levels in  $v = 0$  following quenching of the  $v = 1, j = 0$  level of CO in collisions with H.
- Fig. 6. Distributions of final rotational levels in  $v = 0$  following quenching of the  $v = 1, j = 0$  level of CO in collisions with H.
- Fig. 7. Distributions of final rotational levels in  $v = 0$  following quenching of the  $v = 1, j = 1$  level of CO in collisions with H.

- Fig. 8. Distributions of final rotational levels in  $v = 0$  following quenching of the  $v = 1, j = 2$  level of CO in collisions with H.
- Fig. 9. Rate coefficients for the quenching of the  $v = 1, j = 0, 1$  and  $2$  levels of CO in collision with H as functions of the temperature: solid line —  $j = 0$ , dotted line —  $j = 1$ , dashed line —  $j = 2$ , solid circle — IOS results [17].
- Fig. 10. Cross sections for the rotational quenching of  $v = 1$  level of CO in collisions with H as functions of collision energy: solid line —  $j = 1 \rightarrow j' = 0$ , dotted line —  $j = 2 \rightarrow j' = 0$ , dashed line —  $j = 2 \rightarrow j' = 1$ .
- Fig. 11. Rate coefficients for the rotational quenching of  $v = 1$  level of CO in collisions with H as functions of the temperature: solid line —  $j = 1 \rightarrow j' = 0$ , dotted line —  $j = 2 \rightarrow j' = 0$ , dashed line —  $j = 2 \rightarrow j' = 1$ .

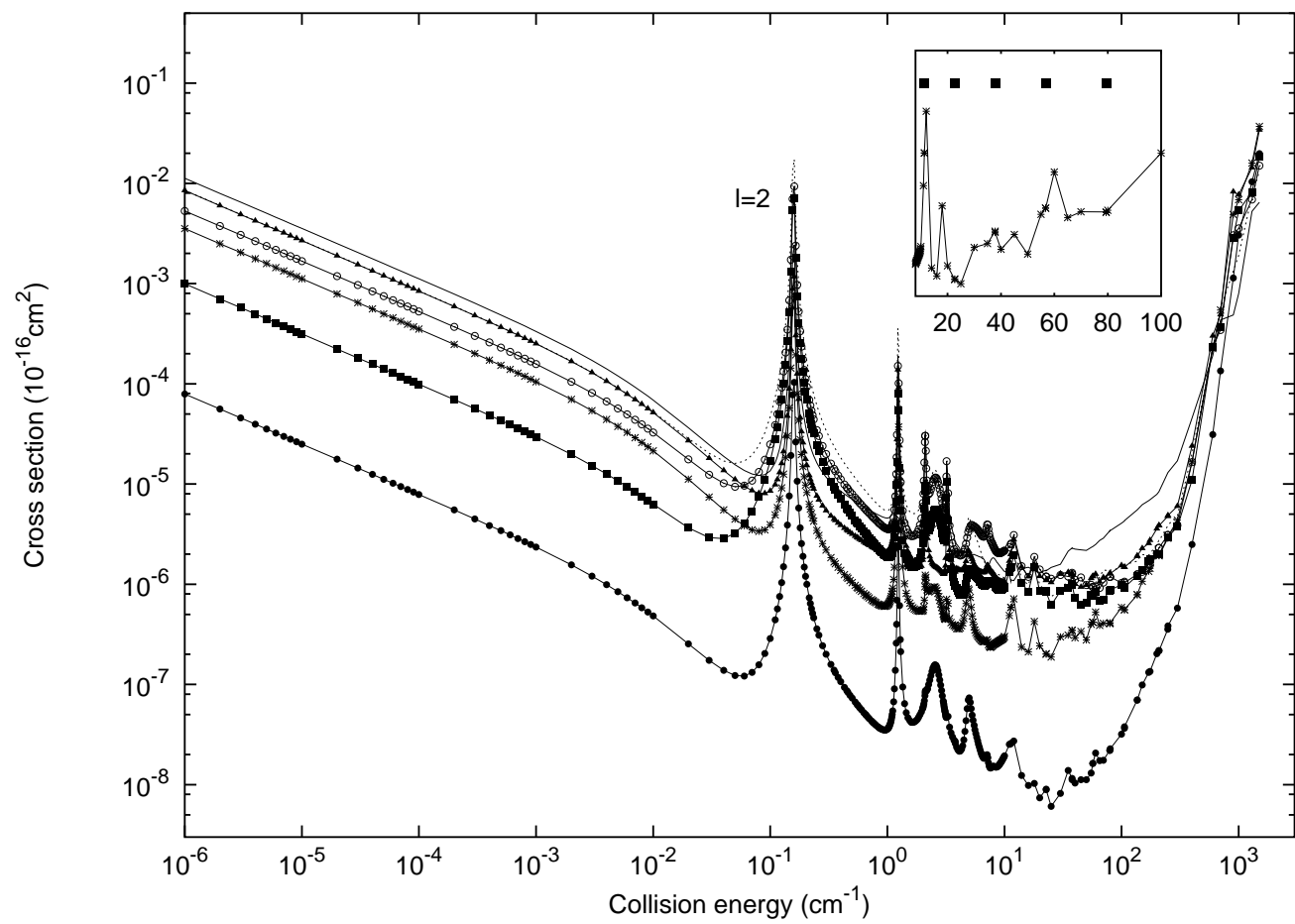


Fig. 1

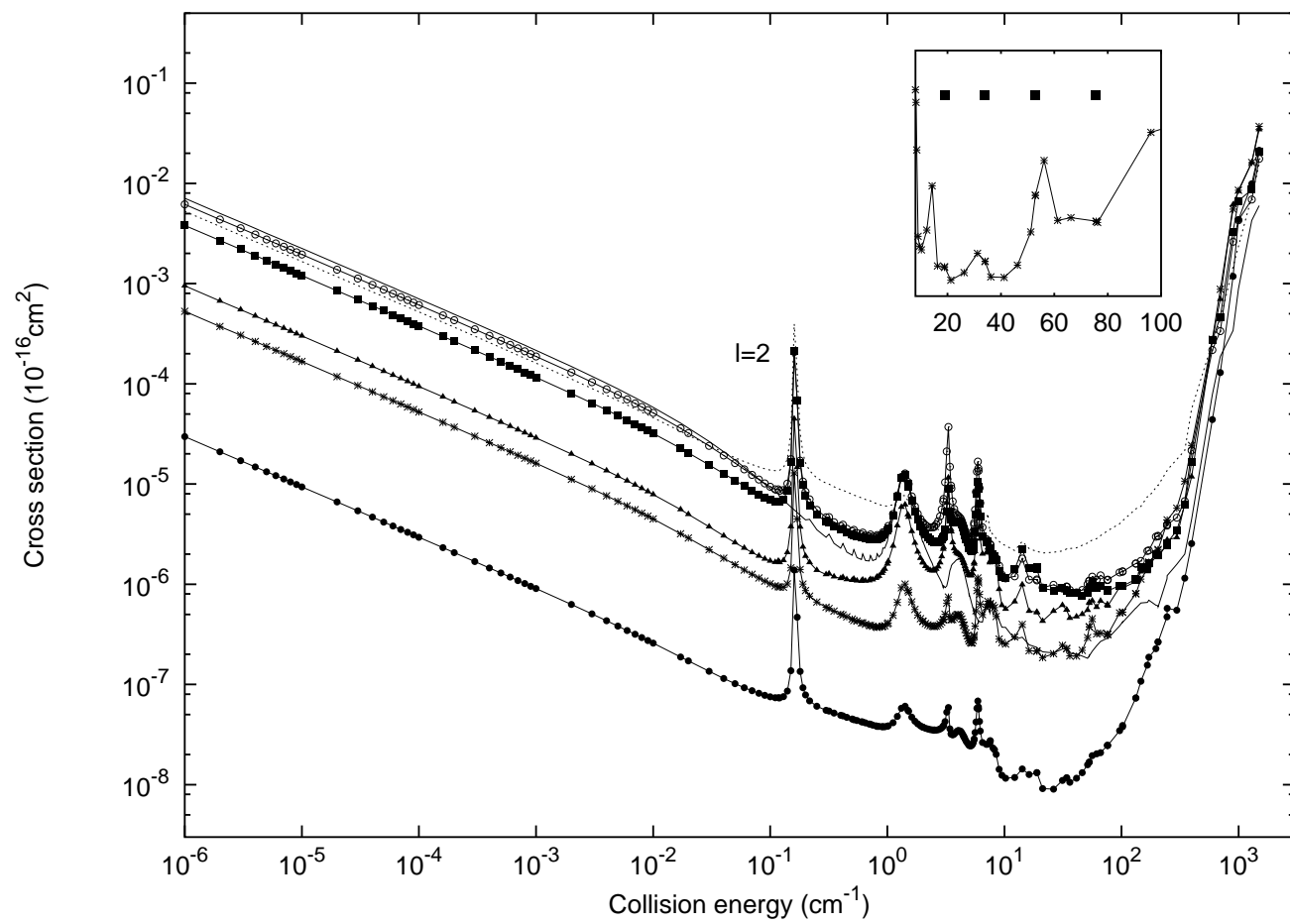


Fig. 2

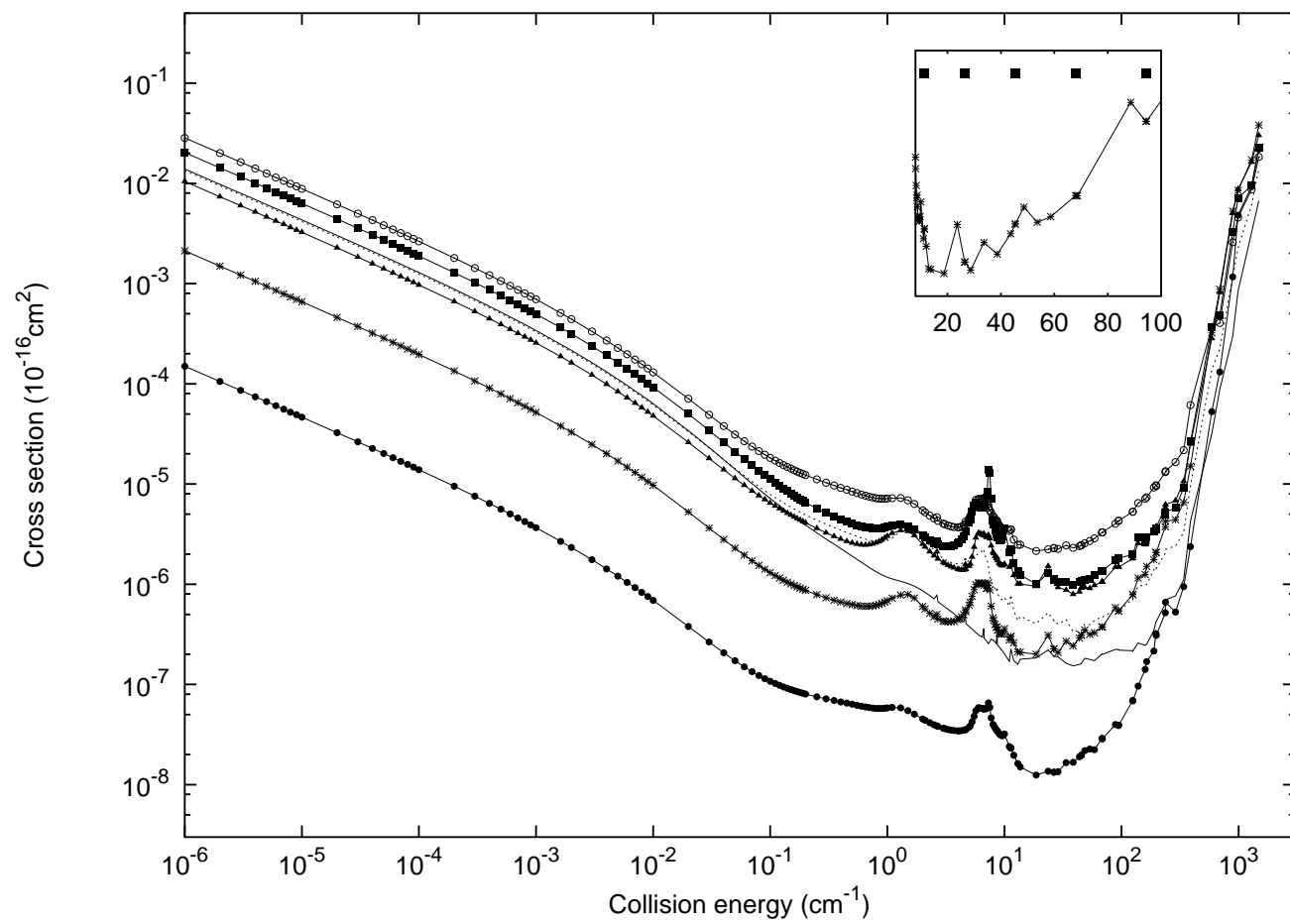


Fig. 3

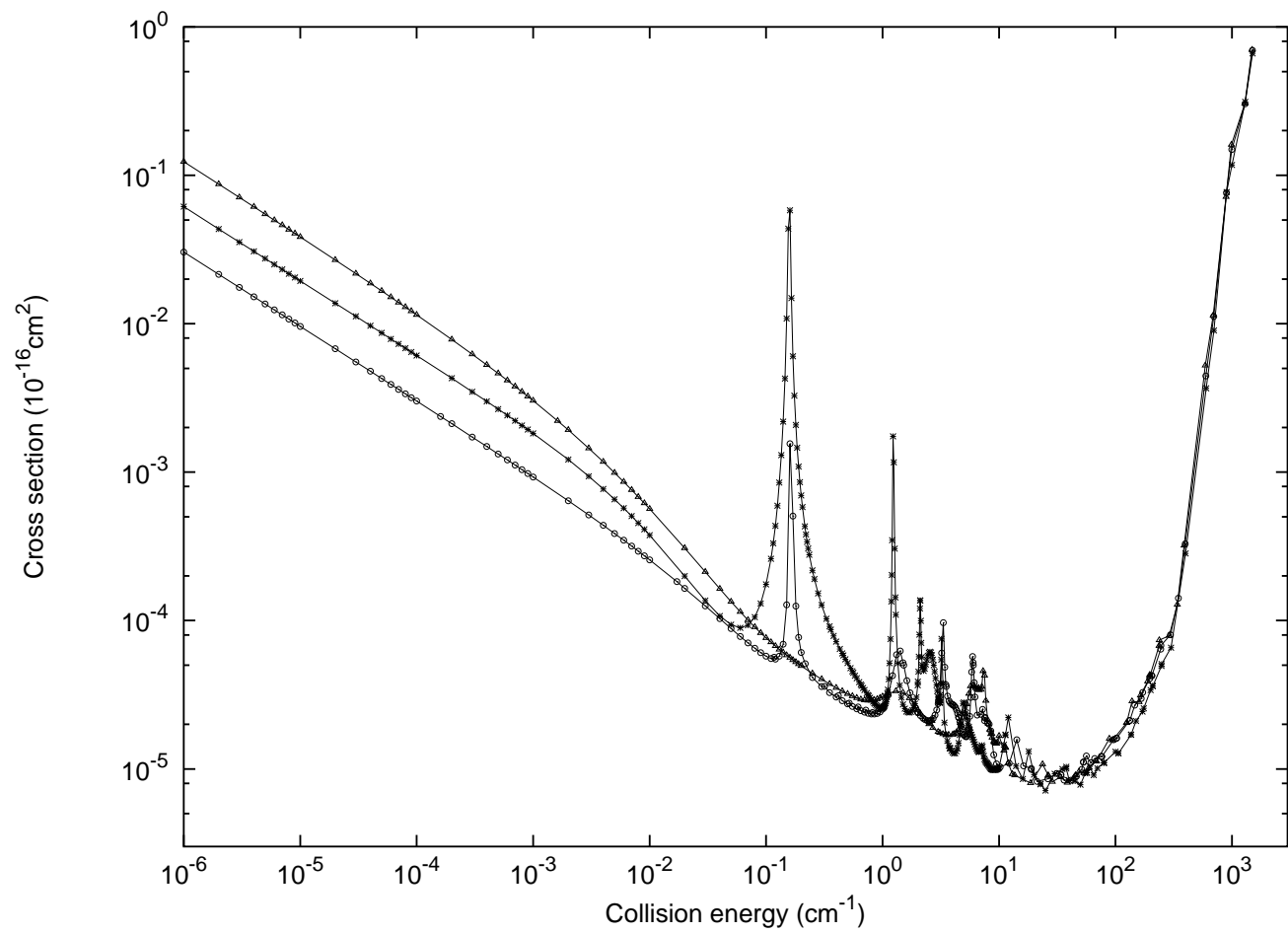


Fig. 4

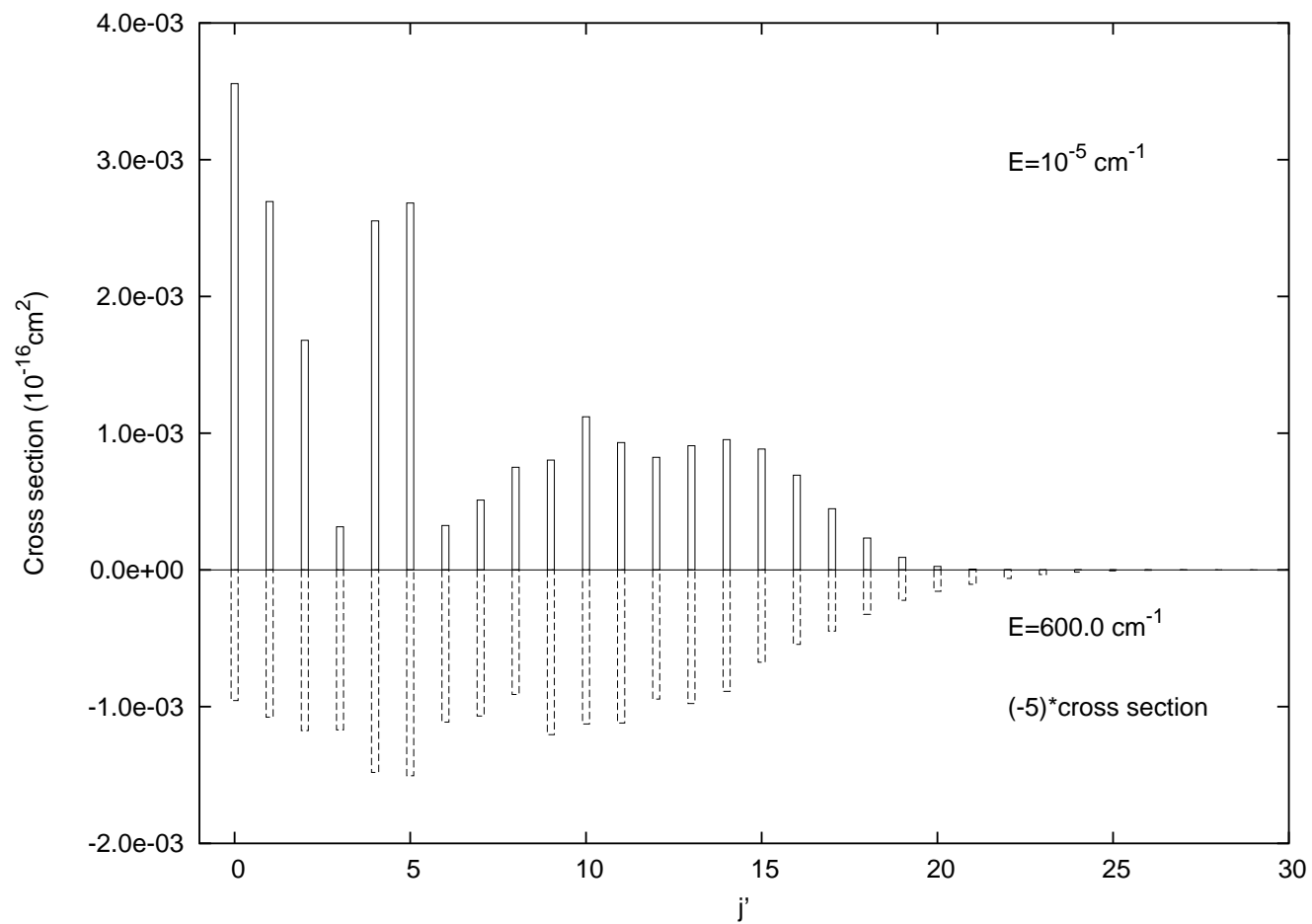


Fig. 5

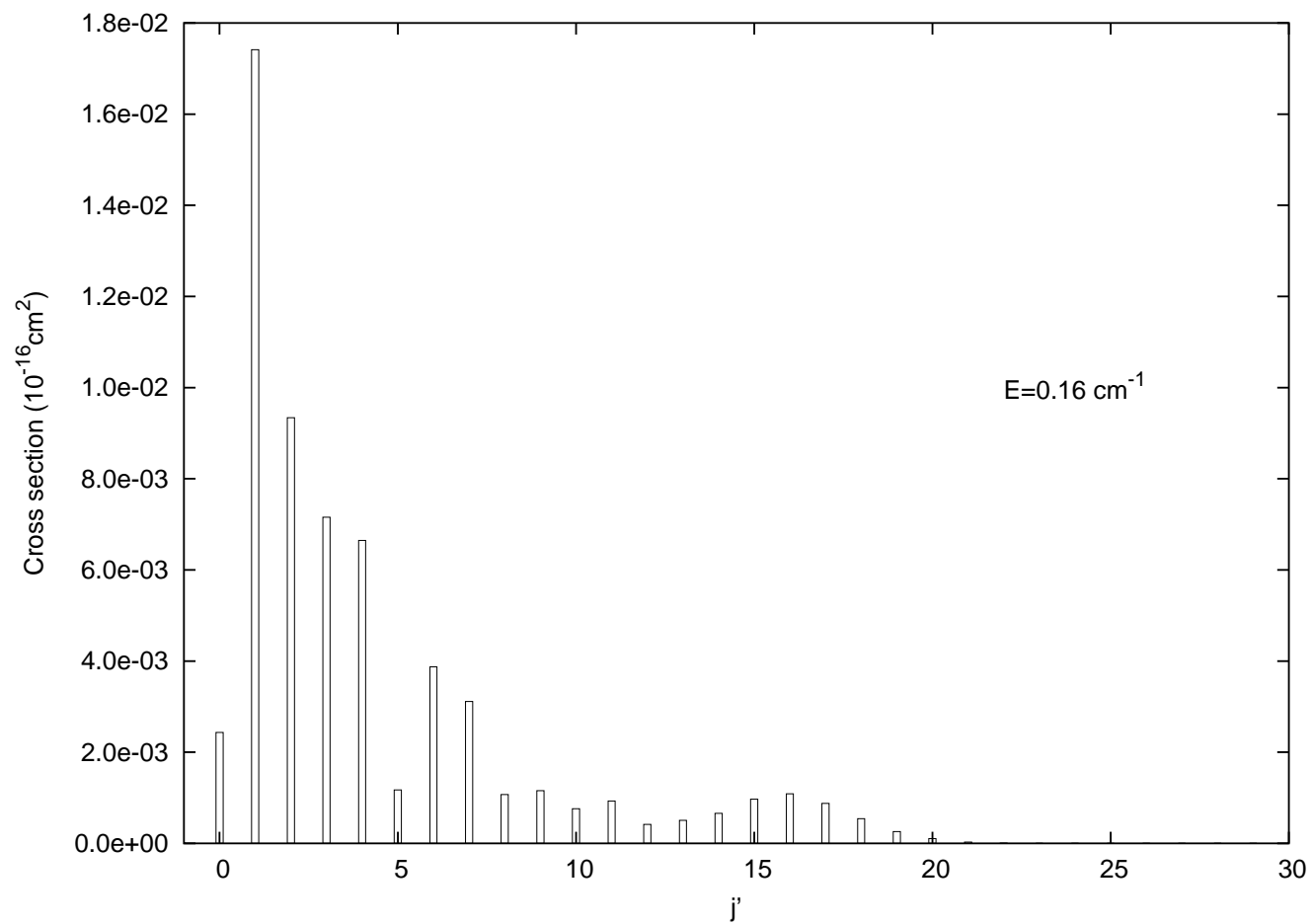


Fig. 6

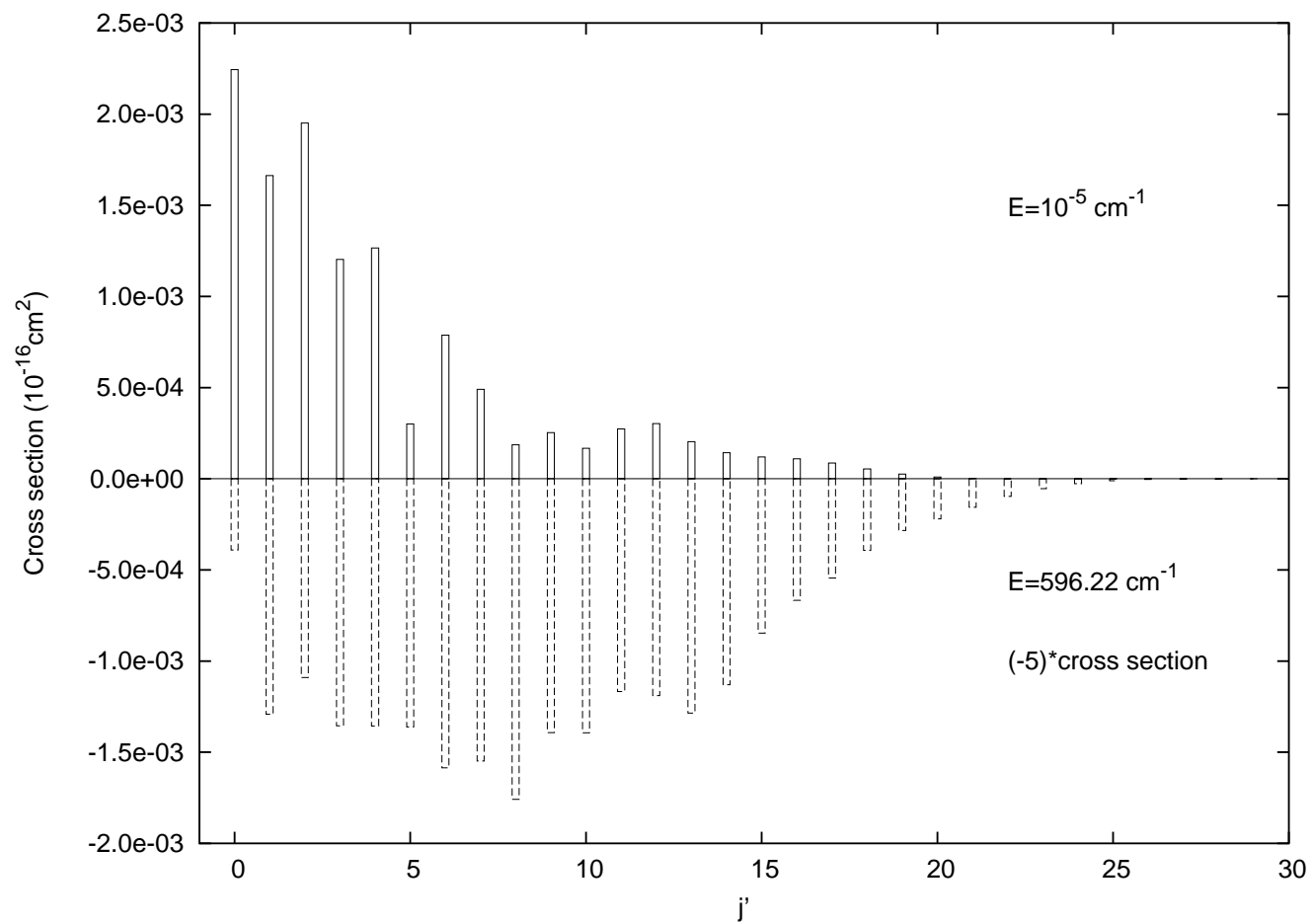


Fig. 7

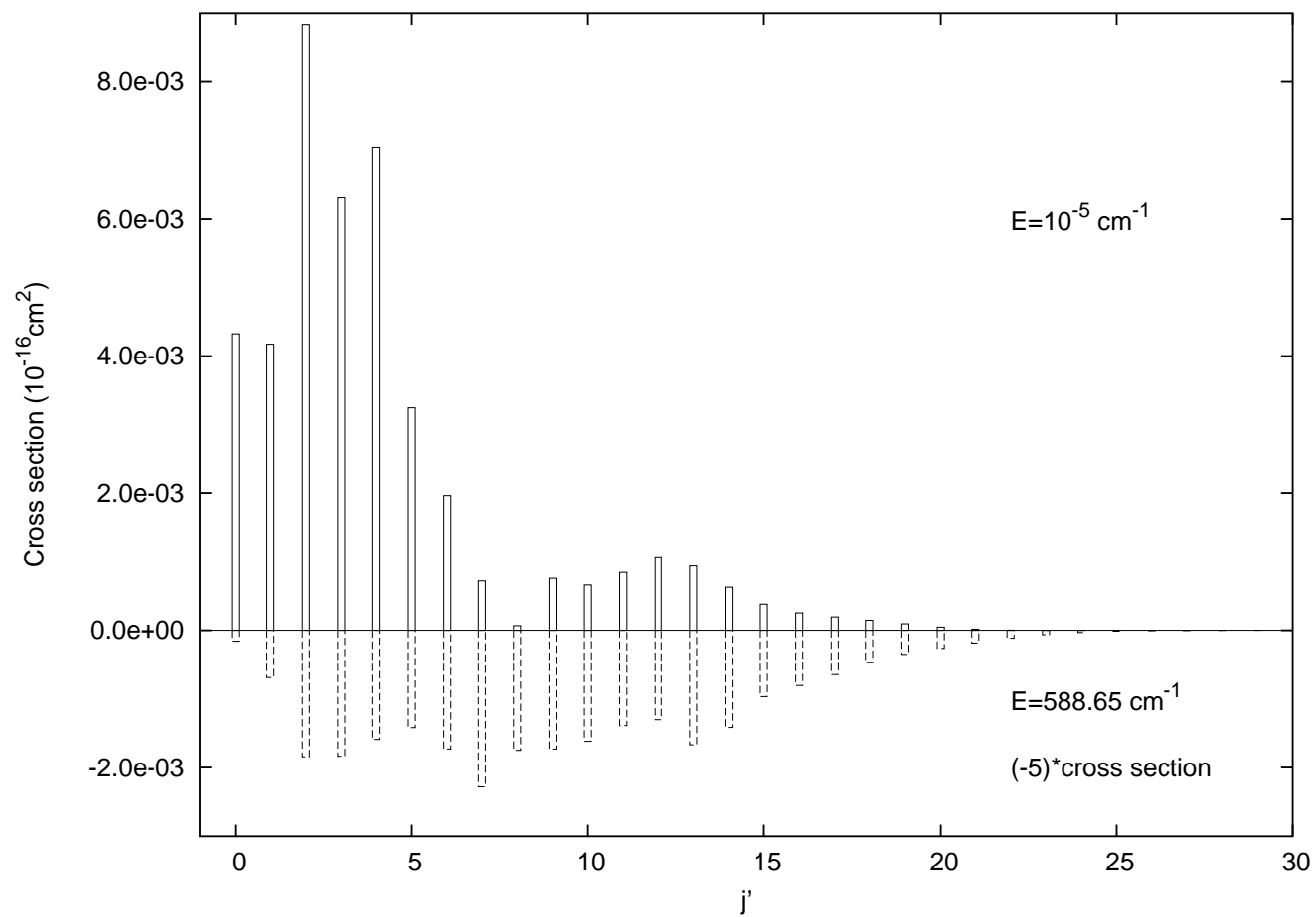


Fig. 8

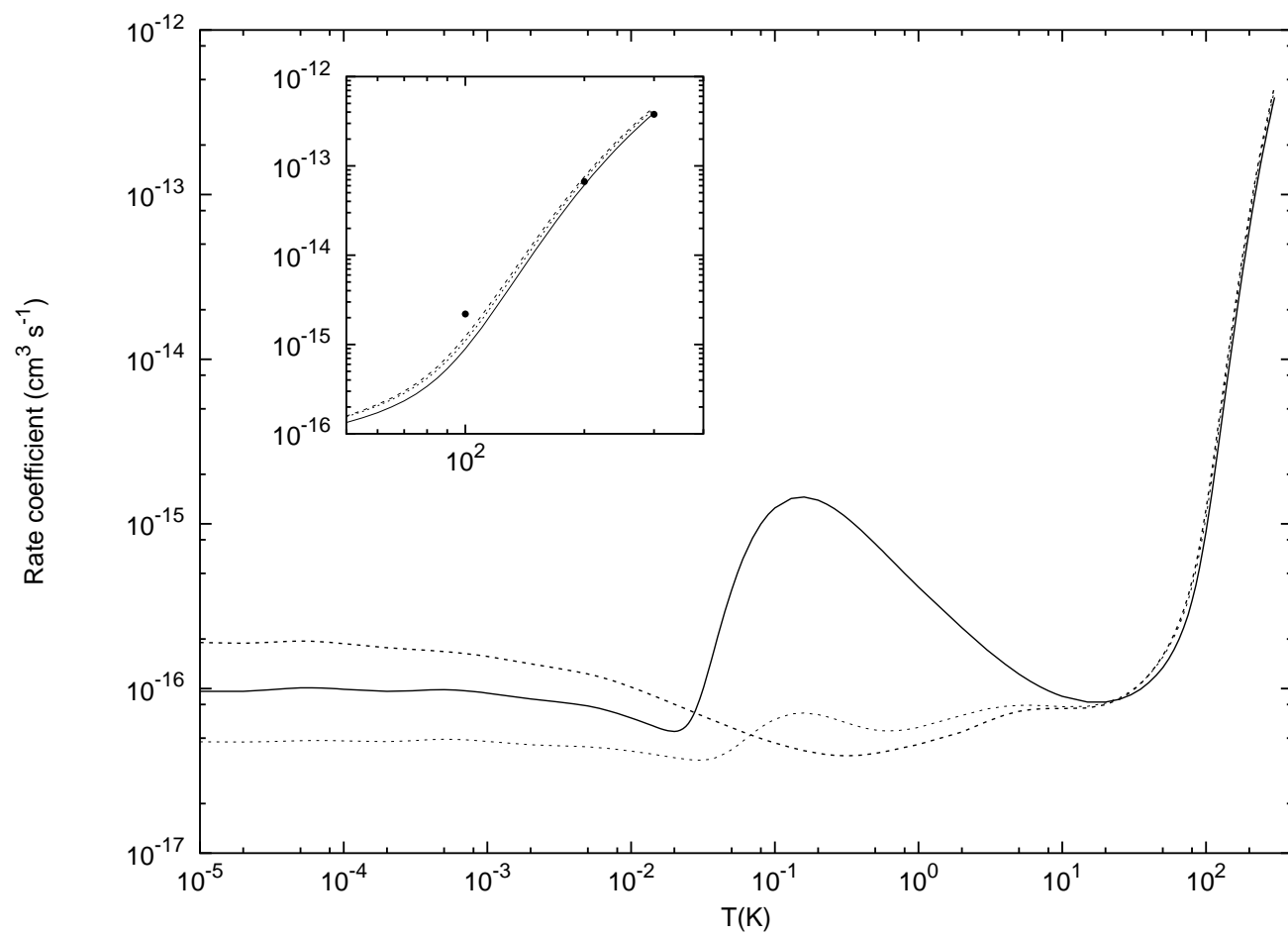


Fig. 9

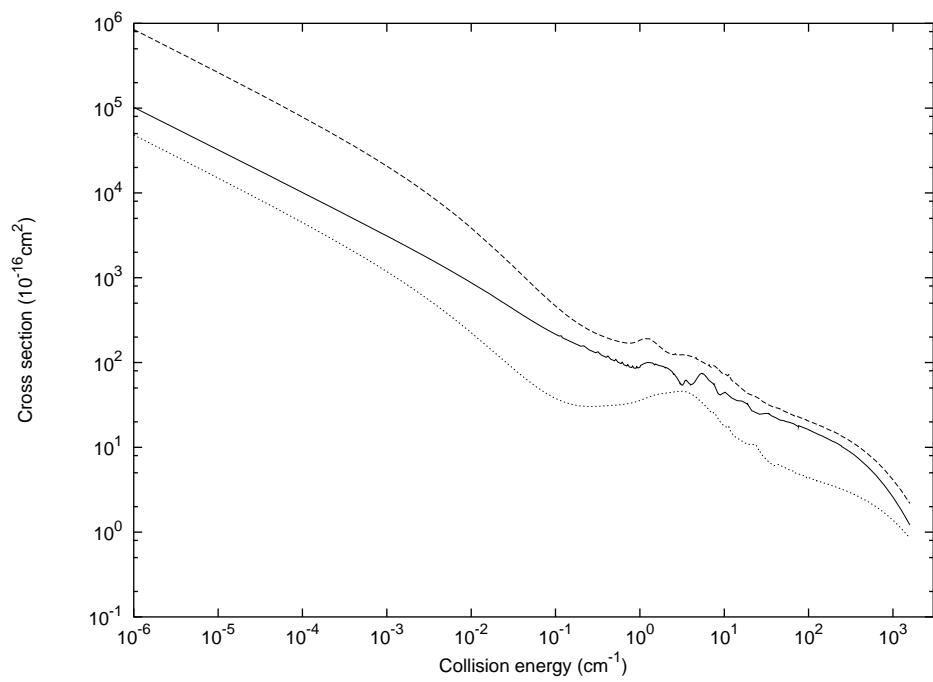


Fig. 10

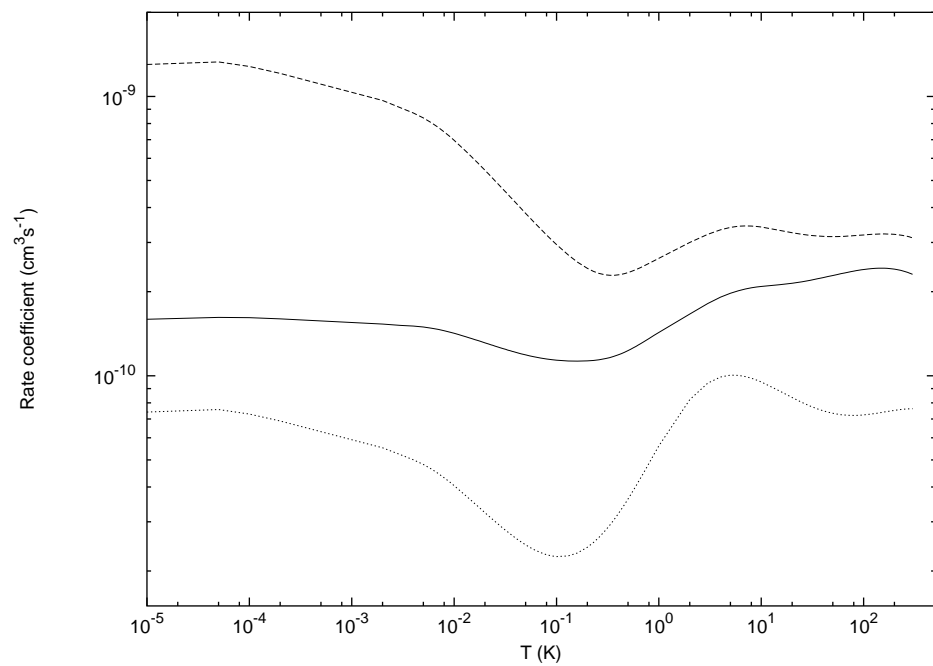


Fig. 11